Robotica (1997) volume 15, pp 275–281. Printed in the United Kingdom © 1997 Cambridge University Press

Intelligent seam tracking using ultrasonic sensors for robotic welding

Ajay Mahajan* and Fernando Figueroa†

(Received in Final Form: August 12, 1996)

SUMMARY

This paper presents a novel approach for seam tracking using ultrasonics. An ultrasonic seam tracking system has been developed for robotic welding which tracks a seam that curves freely on a two-dimensional surface. The seam is detected by scanning the area ahead of the torch and monitoring the amplitude of the waves received after reflection from the workpiece surface. Scanning is accomplished by using two ultrasonic sensors (a transmitter and a receiver) mounted on a stepper motor such that the transmitter angle is the same as the receiver angle. The motor is mounted on the end-effector just ahead of the welding torch and covers a ninety degree arc in front of the torch. If there is no seam then the receiver receives most of the transmitted waves after reflection, but if there is a seam then most of the transmitted waves are dispersed in directions other than that of the receiver. The system has been tested and is very robust in the harsh environments generated by the arc welding process. The robustness of the system stems from using various schemes such as time windowing, a waveguide, air and metal shields, and an intelligent sensor manager. This ultrasonic system offers some distinct advantages over traditional systems using vision and other sensing techniques. It can be used to weld very shiny surfaces, and is a very economical method in terms of cost as well as computational intensity. The system can be used to detect seams less than 0.5 mm wide and 0.5 mm deep.

KEYWORDS: Ultrasonic sensors; Seam tracking; Robotic welding.

1. INTRODUCTION

Real-time seam tracking for robotic arc welding has been an active area of research ever since automobile manufacturers started using robots for welding purposes on their assembly lines. The arc-welding process relies heavily on accurate tracking of joint position and orientation for the production of high quality welds. Thermal expansions experienced by the work piece during the welding process as well as work piece positioning give arise to deviations in the ''taught'' path and the actual required path when off-line programming is used for the welding robots. Hence, currently the emphasis is on real-time seam tracking that compensates for all these deviations.

Many seam tracking methods based on mechanical, electrical, sonic, magnetic and optical sensors can be found in the literature.[1–4] The two most popular methods are through-the-arc sensing and vision based systems. The first is based on intelligence gleaned from the welding arc itself, whereas the second utilizes a data source independent from the welding system. Systems for vision assisted seam tracking have been developed using ordinary light[5–7] and laser light.[8] These by far have been the most successful in real-time seam tracking, but most of these methods entail the use of special filters, extensive computational and data handling procedures, and a substantial capital investment.

The arc instabilities that occur with arc welding processes are likely to affect both the methods mentioned above. For through-the-arc techniques, the interference is reflected in fluctuations in the electrical welding arc signals. Some other drawbacks are that the weld must include a weave, there should not be sharp angles or turns, there should be a proper control of the cast and helix properties of the weld wire, and the system's effectiveness is limited by non-ferrous materials. For the optical techniques, the interference is in the form of optical noise from the high intensity fluctuating arc characteristics. Some further drawbacks of vision based systems are that their success is severely limited by optical noise in the form of visual variations such as rust, grease, chalk marks, scale, or simply the surface being extremely polished or shiny. These require extensive pattern recognition algorithms, and often some form of intelligent control.[7] Furthermore, the seam may easily be obstructed due to spatter, fume, or flux, that may make viewing difficult.[9] Sources of illumination also tend to decrease in brightness due to accumulation of dirt from fumes in a welding environment.

The use of ultrasonics is an attractive alternative to using other methods, and their feasibility in real-time seam tracking for welding purposes has been demonstrated.[10,11] Some of the advantages of using ultrasonic systems over vision based systems are that distance measurements tend to be cheaper and faster,

* Department of Mechanical Engineering, Lake Superior State University, Sault Ste. Marie, MI 49783 (USA).
† Department of Mechanical Engineering, Tulane University, New Orleans, LA 70118 (USA).

and its precision is sufficient for most control applications. Ultrasonic devices are lighter and more compact. With adequate shielding, the sensors can easily withstand the harsh welding environments without any degradation in the sensing capabilities. An ultrasonic system has been reported[12] that utilizes both, range information and reflected energy amplitude to perform tracking. It uses one ultrasonic transducer to scan the area of the seam and finds the seam by detecting maximum reflected energy in a scan cycle. It also monitors the distance from the transducer to the seam by time of flight measurements. The basis for detection is then the larger amount of energy reflected from the surface when the transducer is at the 45 degree angle with the horizontal. Hence, this system is highly dependent on the geometry of the weld seam, and works excellently for lap and V-groove joints, but not so well for other types of geometries.

In contrast, the detection scheme used in the system presented in this paper compares the amount of energy reflected from the seam against the energy reflected from the flat surface. Two ultrasonic transducers are used, one as a transmitter and the other as a receiver. No range data is used, since the presence of the seam is simply detected by a sudden decrease in the amount of the received energy after reflection. A flat surface reflects most of the energy back into the reciever through a waveguide, while a seam would tend to dissipate some of the energy. The greatest advantage of this simple scheme is that the system works well for any kind of weld geometry. A prototype was built using this principle and tested by using a PUMA 560 for an actual MIG arc welding process.[13] This system could only detect seams that curved in one direction, hence it had limited practical applicability. The work presented in this paper builds upon the original system, and adds a motorized component to the system that allows the system to detect seams curving freely on a two-dimensional surface. It also adds an intelligent control system that significantly enhances the performance of the overall seam tracking system. Seams as narrow as 0.5 mm have been detected on shiny aluminum plates supplied to the authors from NASA.

Section 2 describes the basic principle of seam detection and the system configuration. Section 3 presents the tracking scheme and the trajectory generating algorithm. Section 4 gives actual experimental results. Section 5 gives some conclusions, recommendations, and some potential future work that will be done.

2. SYSTEM CONFIGURATION

The basic principle used in the system is that if an acoustic wave from a transmitter bounces off a flat surface into a receiver that is oriented such that the angle of incidence of the transmitter is the same as the angle of reflection of the receiver, then most of the energy will be received by the receiver, and any break in this surface (a seam in this case) will disperse or scatter some energy that it will be enough to detect the presence of a seam. A wave guide is used with the receiver to concentrate at a very small region of the surface. Figure 1 shows the behavior of the waves on a flat surface, where most of the energy bouncing off the flat surface enters the waveguide.

Figure 2 shows the basic principle of seam detection with various seam geometries. It can be seen that at least some of the energy is scattered thereby ensuring that the energy received by the receiver would be less than that received when there is no seam.

Scattering will occur if the seam directs the waves in a direction different than that of the receiver (e.g. V-shaped weld seam—Figure 2(a)), or if the aperture of the seam is greater than the wavelength of the wave (e.g. Butt weld seam—Figure 2(b)), or the seam geometry is such that even though the angle of reflection is the same it is shifted such that very little energy enters the waveguide (e.g. Lap joint type of seam—Figure 2(c)).

A wave guide has been used to improve the resolution of the acoustic signal detected and to eliminate noise coming from all directions with exception of the region to which the waveguide is aimed.[13] The waveguide improves the resolution of the detection scheme in three ways. First, it allows to aim to a small region of interest, comparable to the largest diameter of the seam, by getting close to it. Thus, more energy travels along the waveguide to the receiver, thereby improving the signal to noise (S/N) ratio. Second, if properly dimensioned, the waveguide can perform as a resonator such that the pressure felt at the receiver is increased, again increasing the signal to noise ratio. Third, the waveguide can also

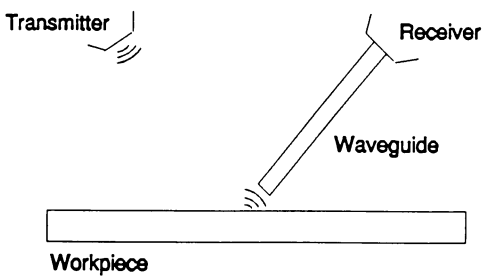

Fig. 1. Waves bouncing off a flat surface.

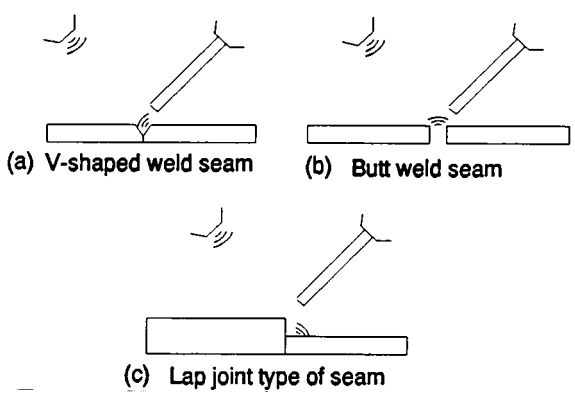

Fig. 2. Basic principle of seam detection for various seam geometries.

be used as a filter since acoustic waves oscillating at the resonant frequency are enhanced and the other waves are diminished. The waveguide was completely re-designed from the original prototype, and was developed such that its length could be changed during run-time.

The transmitter and receiver were mounted on a fixture which allowed the angle of incidence and reflection to be changed to obtain optimum operating configuration during experiments. The fixture was mounted on a stepper motor, and the whole assembly can be mounted on the robot end effector just ahead of the welding torch (see Figure 3). The distance between the torch tip center and the motor center is defined as L, and the distance between the motor center and the center of the waveguide is defined as the scan radius R. Both can be changed by minor adjustments to the hardware assembly.

The signal received by the receiver through the waveguide is processed to generate TTL level signals. A TTL "high" indicates that the acoustic energy received is higher than the threshold, signifying the presence of a flat surface. When the received energy level falls below the threshold value, a TTL "low" signifies the presence of a seam. A *time window* synchronized to the received pulse is generated using timing and logic circuits. This time window is utilized to sample the received signal only while the received pulse is expected to arrive. Implementation of this time window is very simple in this application since the torch is maintained at a constant height from the work piece, and it is easy to calculate the expected time of flight (TOF) of the reflected wave based on the speed of sound. This improves the reliability of the system by rejecting noises outside this interval. The ultrasonic transducers[14] have a 10 degree aperture (beamwidth), without any secondary lobes. The transducers were operated at 150 KHz since the sensors operating at this frequency were the least sensitive to the arc noise along with the appropriate metal and air shielding.[13] The TTL signals are detected on the digital port of the stepper motor driver, "1" for a TTL "high" and "0" for a TTL "low".

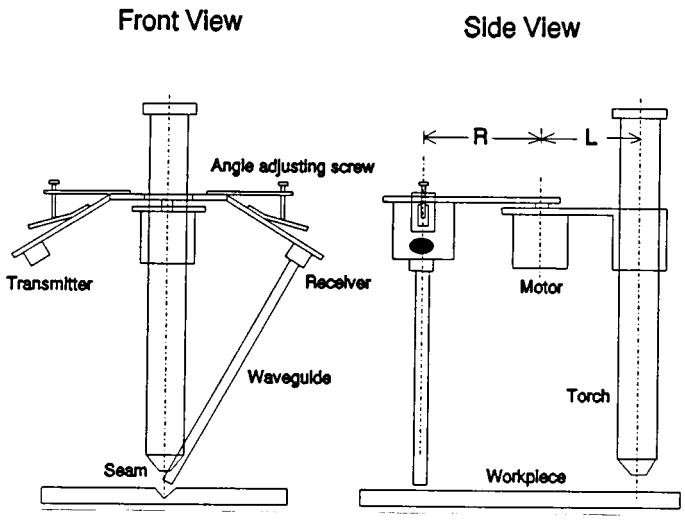

Fig. 3. Stepper motor and sensor assembly.

3. TRACKING ALGORITHM

The system is always started with aligning the sensor assembly along the axis that joins the torch center (T) and the motor center (M), and is referred to as the reference line (see Figure 4). This is done using reference marks on the assembly itself. The system takes this as the reference angle equal to zero degrees for the motor. Any deviation from this line in either direction is called the motor angle denoted as ϕ_M. The system keeps track of this angle through feedback on the number of steps sent by the driver to the motor. The direction is easily known by keeping track of the direction "bit" that is set to run the motor in a particular direction, and is always under the direct command of the *Intelligent Sensor Manager* at the software level. The intelligent sensor manager is an innovative object-oriented module that uses an embedded knowledge base for decision making that significantly enhances the operation of the system at various levels.[15] As soon as a TTL "low" is detected on the digital port, the system automatically records the stepper motor angle ϕ_M.

A TTL "low" will be detected as soon as the waveguide passes over the first edge (point A) of the flat surface and into the seam area, and will continue to detect "low" till it passes over the second edge (point B) on to the flat surface again (see Figure 5).

The number of *zeros* detected by the system depend on the width of the seam and on the update rate of the data acquisition system. The intelligent sensor manager waits for the total number of *zeros* to appear before the next *one,* and then computes the seam position vector based on the middle of the seam (see Figure 6).

As the torch advances, the required shift in translation and orientation (x, y, θ) from one sampled point to the other is determined with respect to the robot base frame. Figure 7 shows the nomenclature for the position vectors in the robot base frame.

The current position of the torch tip is $\mathbf{P}_0$ and $\mathbf{P}_{-1}$ is the previous point visited by the torch. These vectors are with respect to the robot base frame. The tool reference frame is at the torch tip and has a changing orientation based on the curvature of the seam. The x-axis lies along the line joining the torch and the motor center. The orientation is given by the angle θ which is obtained by the slope of the line joining the current and the previous point visited by the torch. This is a strength of the system

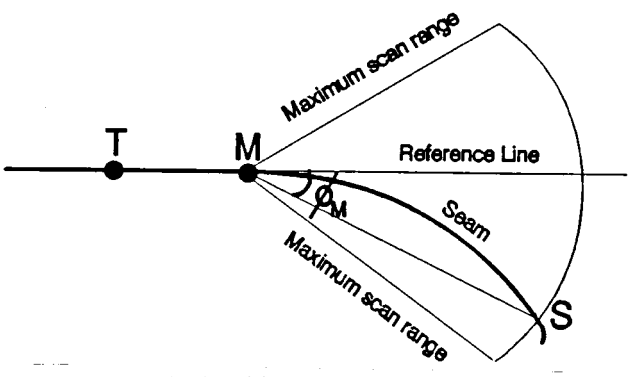

Fig. 4. Motor angle definition.

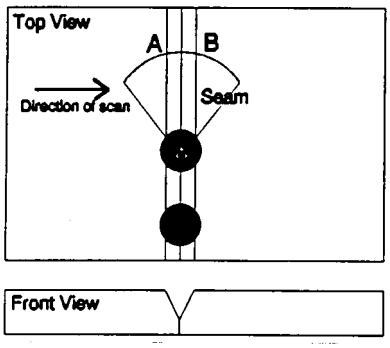

Fig. 5. The role of the seam width in seam detection.

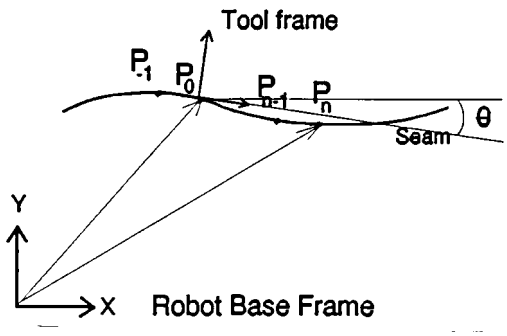

Fig. 7. Position vector nomenclature.

as it allows the robot to follow even sharply curving seams. If the orientation of the tool frame and the robot base frame remained the same throughout the tracking process then this would not be possible. $\mathbf{P}_n$ is the point currently being sampled by the ultrasonic sensors, and $\mathbf{P}_{n-1}$ is the point that was previously sampled. Between $\mathbf{P}_0$ and $\mathbf{P}_n$ are $n-1$ points, which have been sampled previously just as $\mathbf{P}_n$ is about to be sampled.

Assuming that the components of $\mathbf{P}_0$ (Px_0, Py_0, θ_0) are known, the components of $\mathbf{P}_n$ (Px_n, Py_n, θ_n) can be calculated with the help of the developed tracking algorithm. Figure 8 shows the different positions, lengths and angles used to obtain the tracking algorithm. The point T is the current torch position ($\mathbf{P}_0$), point M is the motor position, point S is the current point on the seam being sampled ($\mathbf{P}_n$), and point O is the perpendicular from point S on to the horizontal axis passing through point M. The distance between the torch tip and the motor is L, and scan radius is R. As mentioned earlier, ϕ_M is the angle that the motor has moved for the detection of the seam (in this case since the point is $\mathbf{P}_n$, the angle will be referred to as $\phi_{M,n}$). θ_0 is the angle between the tool reference frame and the robot reference frame at point $\mathbf{P}_0$.

Given the position vector $\mathbf{P}_0$ at point T, one has to calculate the position vector $\mathbf{P}_n$ at point S. The x component of $\mathbf{P}_n$ is given by the sum of the components shown as a, b, and c in Figure 8. Hence ,

$$Px_n = Px_0 + L\cos\theta_0 + R\cos(\phi_{M,n} - \theta_0) \quad (1)$$

and the y component is given by

$$Py_n = Py_0 + L\sin\theta_0 - r\sin(\phi_{M,n} - \theta_0) \quad (2)$$

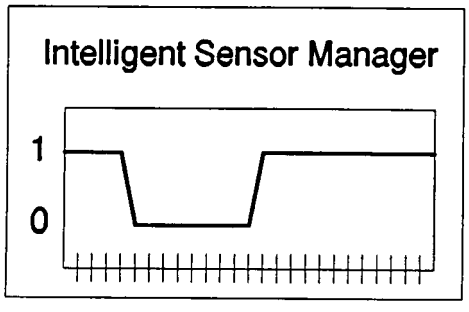

Fig. 6. A snap shot of the seam detection process.

Similarly, equations for the position vector $\mathbf{P}_{n-1}$ may be obtained by the following equations

$$Px_{n-1} = Px_{-1} + L\cos\theta_{-1} + R\cos(\phi_{M,n-1} - \theta_{-1}) \quad (3)$$

$$Py_{n-1} = Py_{-1} + L\sin\theta_{-1} - R\sin(\phi_{M,n-1} - \theta_{-1}) \quad (4)$$

When the torch tip reaches point $\mathbf{P}_{n-1}$, the robot arm must shift by a vector amount

$$\Delta P_n = P_n - P_{n-1} \quad (5)$$

in order to advance to position $\mathbf{P}_n$ in a straight path. Substituting equations (1–4) into equation (5), one can obtain the components of the vector shift $\Delta\mathbf{P}_n$ (ΔPx_n, ΔPy_n, $\Delta\theta_n$) in therms of the known position vectors $\mathbf{P}_0$ and $\mathbf{P}_{-1}$. Hence, ΔPx_n is given by

$$\Delta Px_n = Px_0 - Px_{-1} + L\cos(\theta_0 - \theta_{-1}) + R[\cos(\phi_{M,n} - \theta_0) - \cos(\phi_{M,n-1} - \theta_{-1})] \quad (6)$$

But, $\mathbf{Px}_0 - \mathbf{Px}_{-1} = \Delta\mathbf{Px}_0$, hence, equation (6) can be written as

$$\Delta Px_n = \Delta Px_0 + L\cos(\theta_0 - \theta_{-1}) + R[\cos(\phi_{M,n} - \theta_0) - \cos(\phi_{M,n-1} - \theta_{-1})] \quad (7)$$

The corresponding equations for the y and θ shift are given by

$$\Delta Py_n = \Delta Py_0 + L\sin(\theta_0 - \theta_{-1}) - R[\sin(\phi_{M,n} - \theta_0) - \sin(\phi_{M,n-1} - \theta_{-1})] \quad (8)$$

$$\Delta\theta_n = \theta_n - \theta_{n-1} \quad (9)$$

Equations (7–9) give the computed values for the shift

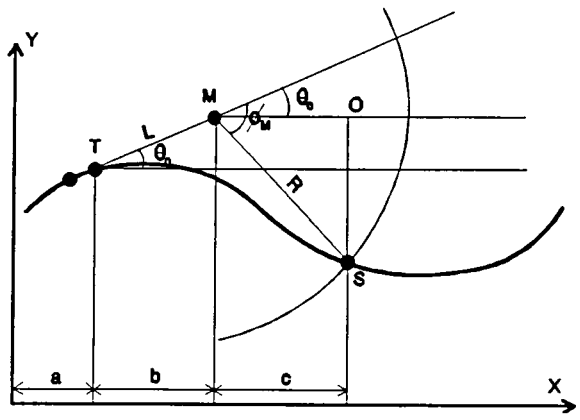

Fig. 8. Tracking algorithm.

of the torch tip from the position $\mathbf{P}_{n-1}$ to $\mathbf{P}_n$ in terms of known parameters. Also, note that these equations are independent of the torch tip position with respect to the robot base frame. However, position feedback is required to monitor the torch tip position and determine when the torch reaches a particular sample point on the seam. The shifts given by equations (7–9) are calculated, and stored in memory until they are required for actual execution. Calculation of the $\Delta\mathbf{P}_n$ can be made just after the robot executes the $\Delta\mathbf{P}_0$ shift, and point $\mathbf{P}_n$ has been sampled.

To start the tracking process the torch tip is taken to a known or taught position, and an inertial reference frame is set up. Initially, the tool frame must be manually aligned with robot base frame. The system is then allowed to start the tracking process by taking the sensors near the seam and allowing it to detect the seam on its own. The welding process is started when the first part of the seam has been sampled and the torch tip has reached the start of the seam.

4. TESTING AND EVALUATION

The focus of this paper is the accuracy obtained by the system in tracking freely curving seams on a two dimensional surface. Furthermore, it will be shown that the system can detect seams less than 0.5 mm wide and 0.5 mm deep on a very shiny aluminum sheet. Hence, the experiments were conducted on an optic table that had motorized linear slides, and had a least count of 0.01 mm. The feasibility of using the system under actual arc welding environments has already been reported.[13] The limitation in that case was the ability to follow the seam in only one direction, and the errors involved in sharply turning curves. The work presented in this paper significantly enhances the operation of the original prototype by innovative changes at the hardware and software level.

The experimental set up is shown in Figure 9, and consists of two orthogonal motorized linear slides with the sensor assembly mounted on top of it. This allows for the x and y movement in the plane of the optic table.

The system was tested on two types of seams. The first was a curving seam (in both directions) milled out on an aluminum plate with typical seam parameters (a V-groove that has 3.175 mm wide and 3.175 mm deep), and the second was an aluminum plate that had an extremely narrow seam (0.5 mm wide and 0.5 mm deep) and would cause some difficulty to a vision system due to its very shiny surface and narrow seam. The torch speed as controlled by the linear slides was 15 mm/sec, and the scanning speed of the stepper motor on the sensor assembly was 20 degrees/sec. The scan radius R was 30 mm, and the length L was 38.5 mm.

Figure 10 shows the first plate that was used for the system evaluation. Note that the seam curves freely in both directions. The system detects the leading and the trailing edge in each scan, and it always returns the coordinates of the center as was described earlier using Figures 5 and 6. Both half circles that were milled have a radius of 5 cm.

Figure 11 shows the results of trackng the seam of plate 1. The errors in the x (solid squares) and y (solid traingles) coordinates are shown. These errors are the deviation of the tracked position as obtained from the linear slides and compared to the known geometric positions of the points on the plate. Again, it is to be noted that the width of the seam is 3.175 mm, hence the errors are taken as the deviation of the tracked position from the center of the two edges as detected by the intelligent sensor manager.

Figure 12 shows the second plate that was used for evaluation purposes. This plate was supplied to the authors by NASA's Johnson Space Center to detect very narrow seams on aluminum plates. This plate really consists of four smaller plates welded together. When the authors received this plate, sections AB and EF were already welded together. Section CD was not welded, and was used as the test seam for the evaluation of the system. The focus of this experiment was not the ability to track curving seams since that was done in the earlier experiment, but was to test the ability of the system to detect and track extremely narrow seams. This particular seam was 0.5 mm wide and 0.5 mm deep. In fact, when the system was used to track this seam, it actually detected the leading and the trailing edge of the seam

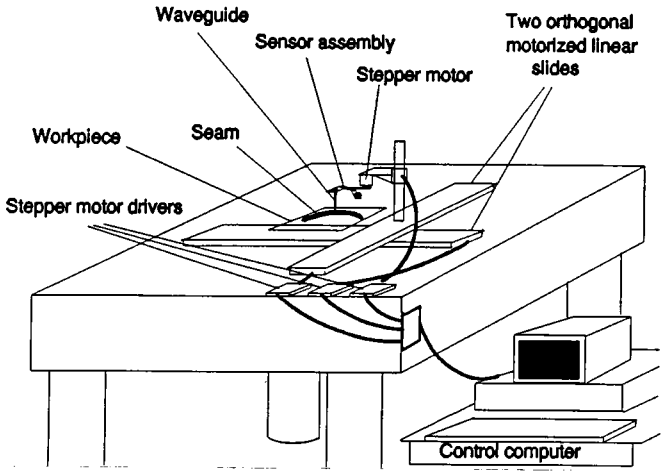

Fig. 9. Experimental set up.

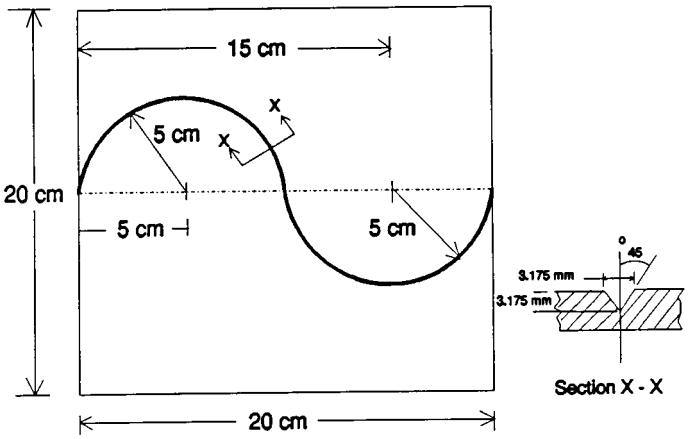

Fig. 10. Plate 1 used in the evaluation process.

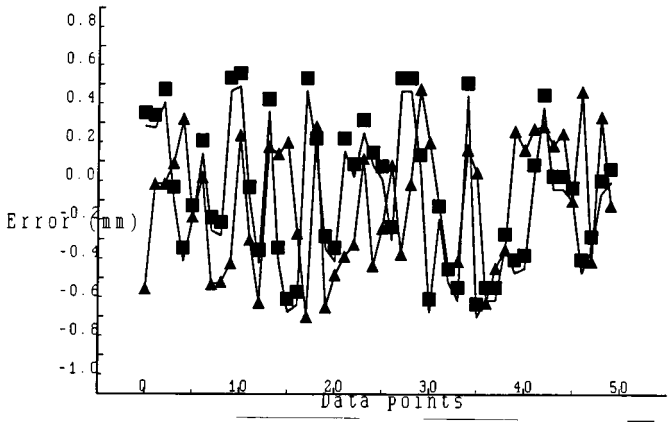

Fig. 11. Errors (in mm) in the seam tracking process for plate 1.

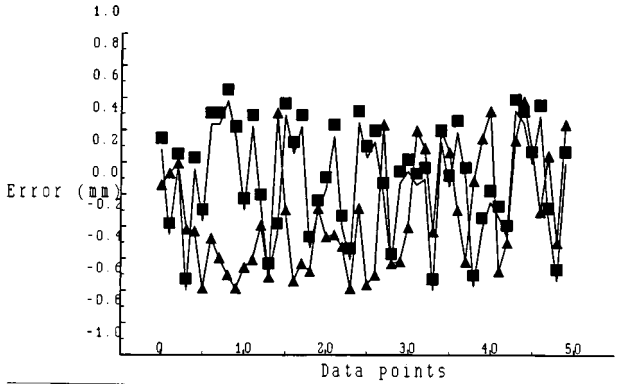

Fig. 13. Errors (in mm) in the seam tracking process for plate 2.

with four data points within, which leads the authors to believe that the system is capable of detecting seams that are as narrow as 0.1 mm.

Figure 13 shows the errors involved in the tracking of the seam on plate 2. Solid squares represent the errors in the x coordinates and solid triangles represent the errors in the y coordinates.

Most of the absolute errors were within $+/-0.5$ mm for both the evaluations as can be seen from Figures 11 and 13. There were some spikes in the original data that were compensated for by using a moving average predictive algorithm in the intelligent sensor manager. More sophisticated tracking algorithm may be used, for example, the extended iterative Kalman filter has been used with great success[7] in a similar seam detecting process using embedded knowledge bases.

5. CONCLUSIONS AND RECOMMENDATIONS

This paper extends a system previously reported[13] to include capabilities such as the detection of freely curving seams in two dimensions, and the detection of seams that may be less than 0.5 mm wide and 0.5 mm deep. The feasibility of the system under actual welding conditions has already been demonstrated, and this paper shows evaluation tests done on an optic table with motorized linear slides to show the accuracy of the system. The system uses two ultrasonic sensors to detect the presence or absence of the seam based on the level of the reflected energy from the work piece. Various innovative schemes such as time windowing, a waveguide, and an intelligent sensor manager have been used to enhance the accuracy of the system. The absolute accuracy of the system has been shown to be within $+/-0.5$ mm. The system is an attractive method for real-time robotic welding since it is simple, economical, fast, accurate, and works on all kinds of seam geometries. Future work entails the ability to track freely curving seams in three dimensions by extracting information about the surface normal. This may entail the use of another motor that would track the surface characteristics.

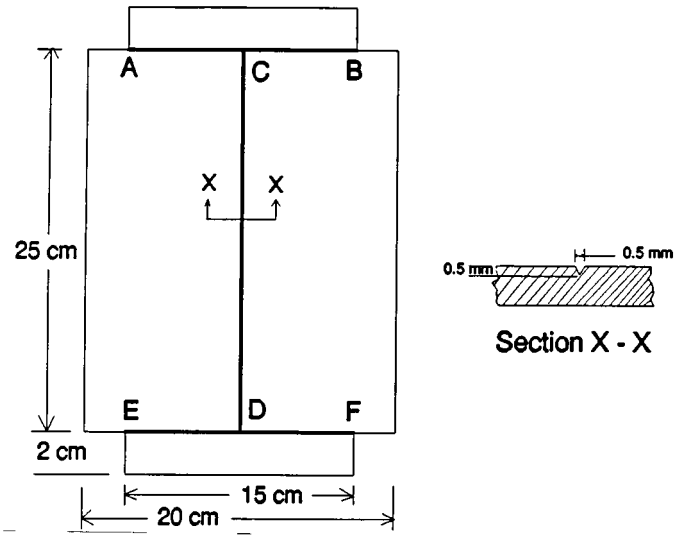

Fig. 12. Plate 2 used in the elevation process.

Acknowledgements

The authors would like to thank Dr. P.M. Lynch and Dr. Evangelis Dousis for their insightful discussions and help on the subject.

References

1. K.W. Brown, "A technical survey of seam tracking methods in welding" *Welding Inst. Rep. 3359,* **1–3,** (1975).
2. S.B. Jones, S.J. Holder and J. Weston, "Mechanical approaches to seam tracking for arc welding" *Welding Inst. Res. Rep.* **167,** (Dec., 1981).
3. G.E. Cook, "Feedback and adaptive control in automated arc welding systems" *Metal Construction* **13,** No. 9, 551–555 (Sept., 1981).
4. R.W. Richardson, "SEAM tracking sensors—Improving all the time" *Welding Des. Fabrication* 77–82 (Sept., 1982).
5. H.E. Smith, W.A. Wall and M.R. Burns, "Automated weld torch guidance control system," Patent #4567384 (assignors to the USA as represented by the Adminstrator of NASA, Washington, D.C., 1986).
6. I. Masaki, "Method and apparatus for manipulator welding apparatus with vision correction for work piece sensing" *Patent* #4380696 (assignor to Unimation, Inc., Danbury, Conn., 1983).
7. J. DePaso and M. Lynch, "Intelligent control with localized/embedded control in an object oriented environment for vision based arc welding" *Proceedings of the ASME,* WAM, Anaheim, CA (1993).
8. R.D. Brown, "Welder with laser TV-scanner" *Patent* #4493968 (assignor to Caterpillar Tractor Co., Peoria, Ill. 1985).

9. J. Hanright, ''Robotic arc welding under adaptive control—a survey of current technology'' *Welding J.* **65,** No 11, 19–24 (1986).
10. E.L. Estochen, C.P. Neuman and F.B. Prinz, ''Application of acoustic sensors to robotic seam tracking'' *IEEE Trans. Ind. Electron.* **IE-31,** No. 3, (Aug. 1984).
11. R. Fenn, ''Ultrasonic monitoring and control during arc welding'' *Welding J.* 18–22 (Sept., 1985).
12. C. Umeagukwu, B. Maqueira and R. Lambert, ''Robotic acoustic seam tracking: System development and application'' *IEEE Trans. Ind. Electron.* **36,** No. 3, 338–348 (August, 1989).
13. F. Figueroa and S. Sharma, ''Robotic seam tracking with ultrasonic sensors'' *Int. J. Robotics and Automation,* IASTED **6,** No. 1, 35–40 (1991).
14. Massa Products Corporation, 280 Lincoln Street, Hingham, Massachusetts 02043.
15. F. Figueroa and A. Mahajan, ''Generic Model of an Autonomous Sensor'' *Mechatronics,* **4,** No. 3, 295–315 (1994).